



# Effect of exposure energy dose on lateral resolution and flexural strength of three-dimensionally printed dental zirconia

Kyle Radomski<sup>1</sup>, Yun-Hee Lee<sup>2</sup>, Sang J Lee<sup>1</sup>, Hyung-In Yoon<sup>3,4\*</sup>

<sup>1</sup>Department of Restorative Dentistry and Biomaterials Sciences, Harvard School of Dental Medicine, Boston, MA, USA

<sup>2</sup>Dental Research Institute, Seoul National University School of Dentistry, Seoul, Republic of Korea

<sup>3</sup>Department of Prosthodontics, School of Dentistry and Dental Research Institute, Seoul National University, Seoul, Republic of Korea

<sup>4</sup>Department of Reconstructive Dentistry and Gerodontology, School of Dental Medicine, University of Bern, Bern, Switzerland

## ORCID

Kyle Radomski

<https://orcid.org/0009-0001-4858-942X>

Yun-Hee Lee

<https://orcid.org/0009-0006-2470-7838>

Sang J Lee

<https://orcid.org/0000-0001-7142-2890>

Hyung-In Yoon

<https://orcid.org/0000-0002-9597-6342>

**PURPOSE.** This study aims to evaluate the effects of exposure energy on the lateral resolution and mechanical strength of dental zirconia manufactured using digital light processing (DLP). **MATERIALS AND METHODS.** A zirconia suspension and a custom top-down DLP printer were used for in-office manufacturing. The viscosity of the suspension and uniformity of the exposed light intensity were controlled. Based on the exposure energy dose delivered to each layer, the specimens were classified into three groups: low-energy (LE), medium-energy (ME), and high-energy (HE). For each energy group, a simplified molar cube was used to measure the widths of the outline ( $X_o$  and  $Y_o$ ) and isthmus ( $X_i$  and  $Y_i$ ), and a bar-shaped specimen of the sintered body was tested. A Kruskal–Wallis test for the lateral resolution and one-way analysis of variance for the mechanical strength were performed ( $\alpha = .05$ ). **RESULTS.** The zirconia green bodies of the ME group showed better lateral resolution than those of the LE and HE groups (both  $P < .001$ ). Regarding the flexural strength of the sintered bodies, the ME group had the highest mean value, whereas the LE group had the lowest mean value (both  $P < .05$ ). The ME group exhibited fewer agglomerates than the LE group, with no distinctive interlayer pores or surface defects. **CONCLUSION.** Based on these findings, the lateral resolution of the green body and flexural strength of the sintered body of dental zirconia could be affected by the exposure energy dose during DLP. The exposure energy should be optimized when fabricating DLP-based dental zirconia. [J Adv Prosthodont 2023;15:248-58]

## Corresponding author

Hyung-In Yoon

Department of Prosthodontics,  
Seoul National University School  
of Dentistry and Dental Research  
Institute, 101, Daehak-ro, Jongro-  
gu, Seoul, 03080, Republic of Korea  
Tel +82220724472

E-mail [drhiy226@snu.ac.kr](mailto:drhiy226@snu.ac.kr)

Received July 7, 2023 /

Last Revision October 2, 2023 /

Accepted October 4, 2023

This study was supported by the Creative-Pioneering Researchers Program through Seoul National University (SNU).

## KEYWORDS

Exposure energy; Dental zirconia; Digital light processing; Lateral resolution; Mechanical strength

© 2023 The Korean Academy of Prosthodontics

© This is an Open Access article distributed under the terms of the Creative Commons Attribution Non-Commercial License (<http://creativecommons.org/licenses/by-nc/4.0>) which permits unrestricted non-commercial use, distribution, and reproduction in any medium, provided the original work is properly cited.

## INTRODUCTION

Zirconia ceramic is a high-strength material with excellent corrosion and wear resistance, which makes it suitable for high-stress environments, such as dental applications from implant fixtures to tooth- or implant-supported fixed prostheses.<sup>1-3</sup> To fabricate accurate dental prostheses with zirconia, subtractive milling (SM) using an optimized tool path has been widely used. However, the inherent drawbacks of SM include the possible risk of microscopic cracks on the surface, waste of leftover blocks, and high consumption of milling tools.<sup>4</sup> Additive manufacturing (AM) has been suggested as an alternative method to fabricate zirconia-based dental prostheses to address the drawbacks of SM.<sup>4-6</sup> Several studies have reported that the flexural strength of AM zirconia is lower than or similar to that of SM zirconia, and the resolution of AM zirconia is comparable to that of SM zirconia, depending on the object geometry or type of test material.<sup>5,7-9</sup>

Among the various existing AM methods, vat polymerization using a light source and photosensitive material can fabricate a product with high resolution, surface quality, and mechanical strength.<sup>10,11</sup> Using stereolithography (SLA) or digital light processing (DLP), a solid ceramic body is generated by successive layering, followed by photopolymerization of a resin-based suspension containing ceramic particles.<sup>4,10,11</sup> It can be used to fabricate complex ceramic structures with high accuracy, surface finish, and process flexibility.<sup>4,12</sup> A DLP technique builds an entire object by stacking each layer from a light-mask image, and the light intensity and exposure time are key production parameters, depending on the characteristics of the suspension.<sup>10,11</sup> During DLP, however, the light scattering of the incident ultraviolet (UV) beam due to the refractory index difference between zirconia powder and photopolymerizable resin has been reported to mainly cause overgrowth of the green body.<sup>10,12,13</sup>

Overgrowth refers to the growth of photopolymerized geometry beyond the dimension of the exposed mask image by scattered light, which is related to low fabrication accuracy.<sup>10,13</sup> A high solid loading of zirconia suspension for dental applications may intensify

scattering, leading to a broadened curing width.<sup>5,13</sup> To reduce scattering, the powder size and mismatch between the monomer and powder should be optimized, minimizing its effect on the curing width.<sup>11,12</sup> The extent of overgrowth of printed zirconia can also decrease significantly by reducing the exposure energy dose, meaning less energy is required to create scattering or affect the curing width.<sup>6,10,14</sup> Sufficient exposure energy to develop a curing depth greater than the layer thickness is necessary for the DLP process.<sup>15,16</sup> Exposure energy may be associated with the homogeneity of polymerization and adhesion between the layers; it can also affect the geometric resolution or internal stress of the green body, and the risk of crack formation or deformation after debinding and sintering.<sup>10,12,15,16</sup> Minimal exposure energy dose with sufficient curing depth and low internal stress was imperative for the DLP of dental zirconia.<sup>15</sup>

The use of DLP with zirconia for dental applications has been reported to be a promising fabrication method.<sup>5,7-9,17-19</sup> However, many aspects such as mechanical properties, aesthetics, and resolution of printed dental zirconia can be affected by the characteristics of suspension, including solid content and particle distribution, and by printing parameters such as layer thickness, build angle, and exposure energy during printing.<sup>5,7,20,21</sup> To date, studies on the effect of exposure conditions (i.e., exposure time or light intensity) on the fabrication quality of zirconia green or sintered bodies generated by DLP for industrial purposes have been reported.<sup>10,14-16,22</sup> However, there are limited studies on the effect of exposure energy on the lateral resolution of green bodies and the mechanical properties of sintered bodies of DLP-generated zirconia for dental applications. This study aimed to investigate the association between the exposure energy and the quality of DLP-generated zirconia for dental applications. This study contributes to the knowledge and advancement of AM for dental materials. The null hypothesis was that there is no difference in the lateral resolution of the DLP-generated zirconia green body and the flexural strength of the zirconia sintered body under different exposure energy dose settings during DLP.

## MATERIALS AND METHODS

A zirconia suspension approved for dental applications (Cera-P; M.O.P, Seoul, South Korea), which consisted of nano-sized 3-mol% yttria-stabilized tetragonal zirconia (3Y-TZP) powder, photopolymerizable binders containing mono- or multi-functional acrylate monomers, a dispersant, and a photoinitiator, was used. The suspension was formulated to initiate radical polymerization around 405 nm wavelength of UV light. The zirconia particles were homogeneously dispersed in the resin mixture for a reasonable period of time for use in the DLP.<sup>7</sup> Since the rheologic behavior of zirconia suspension is important for the resolution of the printed body as well as the recoating process during printing, the apparent viscosity ( $\text{Pa} \cdot \text{s}$ ) of the suspension was periodically measured using a viscometer (DV2T; Brookfield, Middleboro, MA, USA) with a 63-spindle at 40 rpm to monitor the dispersion stability of the tested suspension for DLP. The measurements were performed immediately after suspension preparation (week 0), weekly for up to 4 weeks, and then monthly for up to 7 months (week 28).

A custom cartridge-based DLP printer for zirconia suspension designed for in-office manufacturing of dental prostheses was used in this study, implementing a top-down approach concept, which is useful for a highly viscous resin filled with solid particles to be evenly coated on the build platform.<sup>11</sup> The printer

has a build platform size of 120 mm  $\times$  80 mm, an auto-feeding system with motor pump-driven cartridges, and a recoating metal blade to evenly spread freshly supplied suspension (Fig. 1). A digital micromirror device (DMD) employing a dynamic mask of 4 K (3840  $\times$  2160 pixels) UV light with a wavelength of 405 nm and a pixel size (x-y resolution) of 40  $\mu\text{m}$  was installed as a power source to guarantee high resolution. For the zirconia printing process, the movement speed of the recoating blade was set as 150 mm/s and the thickness of each layer as 50  $\mu\text{m}$ .

Prior to printing, the uniformity of the exposed light intensity on the printer build platform was measured using a UV energy meter (LS133; Linshang, Shenzhen, China). The platform exposed to the UV beam was divided into six identical regions, and the amount of beam irradiation in each region was evaluated (Fig. 2). After verifying the constancy of the light intensity at 50  $\text{mW}/\text{cm}^2$ , three different exposure times (1, 3, and 6s) were tested to assess the effect of the overall exposure energy dose delivered to each printed layer on the lateral resolution of the DLP-generated zirconia green body and on the flexural strength of the sintered body. The overall energy dose for each layer was calculated as follows: overall exposure energy dose ( $\text{mJ}/\text{cm}^2$ ) = light intensity ( $\text{mW}/\text{cm}^2$ )  $\times$  exposure time (s). The specimens were classified into three groups: low-energy (LE, 50  $\text{mJ}/\text{cm}^2$ ), medium-energy (ME, 150  $\text{mJ}/\text{cm}^2$ ), and high-energy (HE, 300  $\text{mJ}/\text{cm}^2$ ) groups.

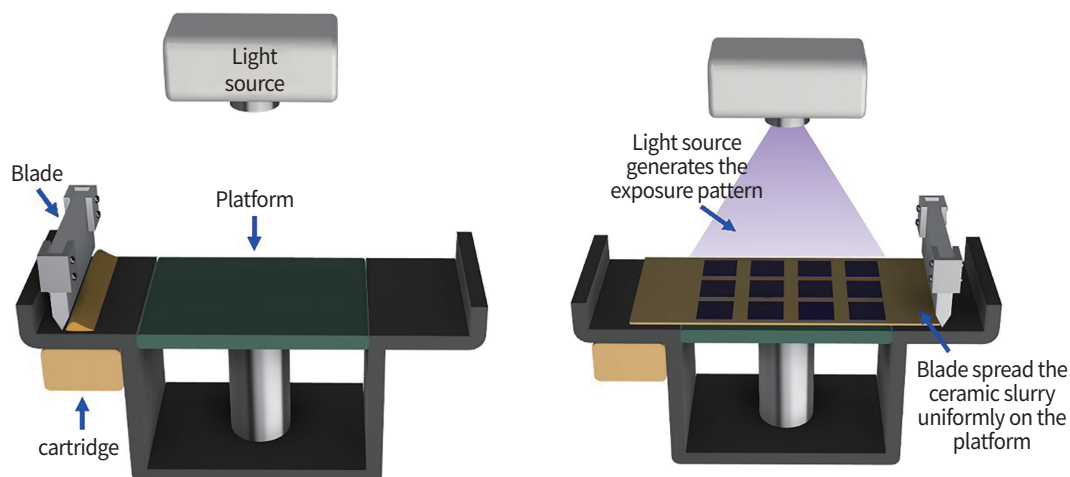
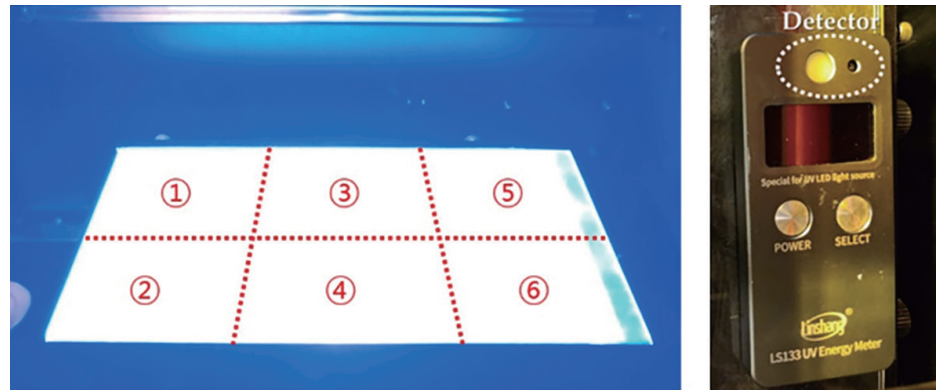


**Fig. 1.** Schematic diagram of the mechanism of a cartridge-based custom printer for digital light processing of dental zirconia suspension with top-down approach. An auto-feeding system with a motor pump-driven cartridge and a recoating blade to evenly spread fresh suspension were implemented.

**Fig. 2.** Uniformity of exposure intensity onto platform was monitored using an ultraviolet (UV) energy meter. Exposed platform by UV light was divided into six identical areas (1 to 6), and beam irradiation amount for each region was evaluated.



To facilitate the linear dimension measurement of the printed body of dental zirconia, a 3D geometric cubic shape stacked in a simplified four-cusped molar form was virtually designed using a software program (Rhino 3D; McNeel Europe SL, Barcelona, Spain), stored as a reference model in a standard tessellation language (STL) file format, and used for printing a green body for analysis (Fig. 3). For the lateral resolution analysis of the printed green body, two different outcomes were evaluated for each energy group: 1) the outline width ( $X_o$  and  $Y_o$ ) in the horizontal plane ( $x$ - and  $y$ -axis) of the cubic shape, originally designed as 12.0 mm in the reference model per axis, and 2) the isthmus width ( $X_i$  and  $Y_i$ ) in each axis of the cubic

shape, originally set to 4.0 mm in the reference model. After fabrication using a custom DLP printer and cleansing with ethanol, four different widths ( $X_o$ ,  $Y_o$ ,  $X_i$ , and  $Y_i$ ) of each cubic green body fabricated under each exposure energy-dose condition were measured using a digital caliper (Digital Caliper Gauge; Mitutoyo, Kanagawa, Japan). To measure the amount of horizontal ( $x$ - and  $y$ -axis dimensions) overgrowth and calculate the lateral resolution of the DLP-generated green bodies, the width measurements were compared with the setting values of the reference model. In this study, the lateral resolution was defined as the numerical difference between the measured width ( $X_o$ ,  $Y_o$ ,  $X_i$ , and  $Y_i$ ) of the printed green body and the origi-

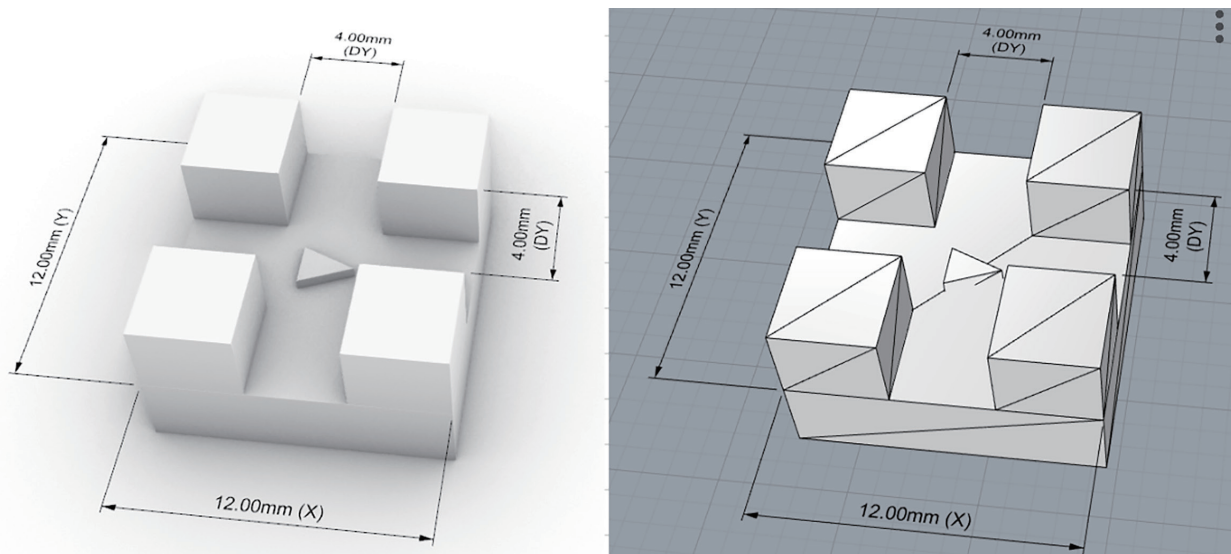


**Fig. 3.** A geometric cubic shape stacked in the simplified four-cusped molar form to measure lateral resolution of zirconia green body manufactured by digital light processing. Two different outcomes were evaluated: 1) outline width ( $X_o$  and  $Y_o$ ) in horizontal  $x$ - and  $y$ -axis of cubic shape (marked as 'X' and 'Y'), originally designed as 12.0 mm per each axis, and 2) isthmus width ( $X_i$  and  $Y_i$ ) in each axis of the cubic shape (marked as 'DX' and 'DY'), originally as 4.0 mm.

nal width of the reference model.<sup>10,23</sup> If the measured value was larger than the reference setting value, it was marked as positive (+); otherwise, it was marked as negative (-).<sup>23</sup>

After measuring the green body, post-processing with heat treatment was conducted to remove the organic materials without creating any undesirable defects, such as delamination, surface cracks, or distortion. First, the weight loss of the green body was monitored as a function of temperature using thermogravimetry and differential thermal analysis (TGA-DTA) (Q50; TA Instruments, New Castle, DE, USA). The zirconia green body was heated to 560°C with a heating rate of 10°C/min in the air atmosphere. As remarkable exothermic peaks were observed at ~250°C and ~430°C, indicating the degradation of polymeric binders, a stepwise debinding and sintering schedule was applied. A slow heating rate of 1°C/min had been applied to prevent any damage to the zirconia brown body. Debinding and sintering of the zirconia green body were performed using a sintering furnace (674i; Dekema, Freilassing, Germany) with the heating schedule depicted in Figure 4.

According to the protocol established by the International Organization for Standardization (ISO) for testing ceramic materials in dentistry (ISO 6872:2015), a bar-shaped specimen (3 mm × 4 mm × 40 mm)

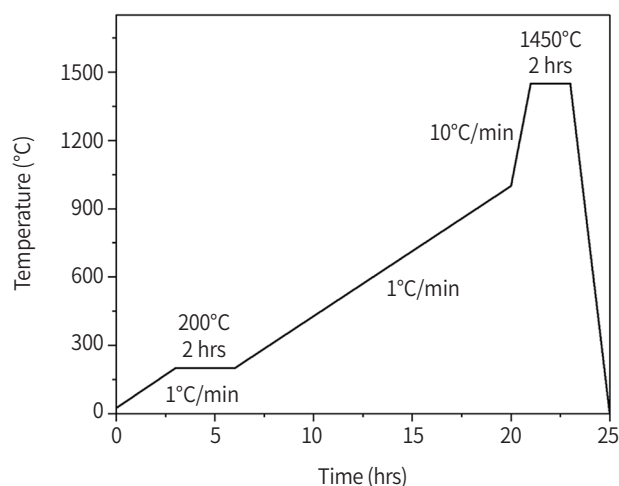


**Fig. 4.** Debinding and sintering schedule for zirconia green body manufactured by digital light processing. A slow heating rate of 1°C/min is applied to prevent any damages on brown body of dental zirconia specimen.

was designed for testing and stored in the STL format. Using a custom DLP printer and the 3Y-TZP suspension approved for dental use (Cera-P; M.O.P, Seoul, South Korea), three different exposure times (1, 3, and 6 s) with a constant light intensity of 50 mW/cm<sup>2</sup> were applied to fabricate zirconia green bodies. Based on the pilot test, the scaling factor was applied for the design according to the estimated shrinkage rate after sintering, 25% ± 1% in every direction. After printing and subsequent cleansing with ethanol, the specimens were debinded and sintered using the aforementioned heating schedules. Thirty bar-shaped specimens were divided into three test groups (n = 10 per group) based on the exposure energy dose (LE, 50 mJ/cm<sup>2</sup>, ME, 150 mJ/cm<sup>2</sup>, and HE, 300 mJ/cm<sup>2</sup>).

After the sintered body was produced, a three-point bending test was performed on each specimen using a universal testing machine (Instron 8871; Instron, Norwood, MA, USA) with a 10 kN load cell at a cross-head speed of 1 mm/min. The flexural strength (FS) was calculated using the following equation:

$$FS = \frac{3P_{max} l}{2bd^2}$$

where  $P_{max}$  is the maximum load before the fracture,  $l$  is the distance between the supports,  $b$  is the specimen width, and  $d$  is the specimen thickness. After failure, three representative specimens from each group (A, B, and C) were collected and examined using a field-emission scanning electron microscope (Apreo S; Thermo Fisher Scientific, Waltham, MA, USA) to analyze the fractured surface of each specimen in terms of porosity or defects. The observed surface was sputter-coated with platinum (Pt), and the accelerating voltage for microscopic examination was set to 10 kV.

Descriptive statistics were calculated using the means and standard deviations of lateral resolution and flexural strength measurements. Based on the results of the Shapiro-Wilk and Levene tests for normality, a nonparametric Kruskal-Wallis test was conducted to compare the calculated lateral resolution; one-way analysis of variance (ANOVA) test was used to compare the flexural strength measurements. Post-hoc pairwise comparisons were performed using the Bonferroni method. All data were analyzed using a statistical software program (Stata BE 17.0; Stata Corp., College Station, TX, USA) ( $\alpha = .05$ ).

## RESULTS

The apparent viscosity (Pa·s) of the prepared zirconia suspension is presented in Figure 5. The values were in the range of 2,349 Pa·s (minimum) to 2,407 Pa·s (maximum), with a small variation between the measurements at 28 weeks. The mean and standard deviation of the viscosity of the suspension was  $2,381 \pm 21$  Pa·s, which was similar to the viscosity of the suspension initially measured at 0 week.

The measured intensities of the UV light beam on the build platform are listed in Table 1. The expected and measured values of the exposure energy dose delivered to six different regions of the exposed build platform area were similar for each region, indicating the uniformity of the exposed energy during dental zirconia fabrication using the custom printer developed for this study. The average difference in the exposure energy dose between the measured and expected values was 1 mJ/cm<sup>2</sup> for the LE group, 0 mJ/cm<sup>2</sup> for the ME group, and 2 mJ/cm<sup>2</sup> for the HE group.

The means and standard deviations of the calculated lateral resolution values are listed in Table 2. Significant differences were detected among the groups ( $P < .001$ ), and the ME group showed the least mean value of lateral resolution of the printed green body,

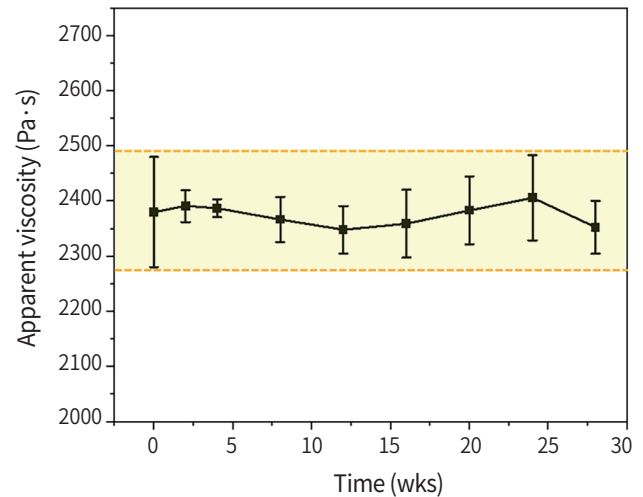


**Fig. 5.** Graph of apparent viscosity (Pa·s) of zirconia suspension, periodically measured to monitor dispersion stability up to 6 months, shows minimal change over time (within the yellow band area).

less than 0.04 mm, showing negative error in  $X_o$ ,  $Y_o$ , and  $X_i$  and null to positive error in  $Y_i$  (all  $P < .001$ ). Regardless of the sign of the calculated value, the LE and HE groups showed significantly greater errors than the ME group; the value was negative for each width in the LE group and positive for each width in the HE group.

**Table 1.** Expected and measured values of exposure energy dose delivered on six different regions of the exposed build platform area during digital light processing

Expected OED (mJ/cm <sup>2</sup> )	Exposed platform area						Measured OED (mJ/cm <sup>2</sup> )
	Region #1	Region #2	Region #3	Region #4	Region #5	Region #6	
50	50	53	51	52	49	51	51 ± 1
150	151	153	148	153	146	149	150 ± 3
300	302	309	301	309	292	297	302 ± 7

OED, overall exposure energy dose.

**Table 2.** Means and standard deviations of lateral resolution of printed zirconia green body. Lateral resolution was calculated as outline width ( $X_o$  and  $Y_o$ ) and isthmus width ( $X_i$  and  $Y_i$ ) in horizontal plane (x- and y-axis) of green body

Group	Outline width		Isthmus width	
	$X_o$	$Y_o$	$X_i$	$Y_i$
Low	(-) 0.103 ± 0.016*	(-) 0.062 ± 0.019*	(-) 0.114 ± 0.030*	(-) 0.127 ± 0.024*
Medium	(-) 0.040 ± 0.021*	(-) 0.014 ± 0.019*	(-) 0.024 ± 0.028*	0.000 ± 0.024*
High	(+) 0.112 ± 0.046*	(+) 0.152 ± 0.046*	(+) 0.052 ± 0.041*	(+) 0.037 ± 0.012*

Low, Low-energy group; Medium, Medium-energy group; High, High-energy group. A statistical significance between the groups was marked with an asterisk (\*).

Means and standard deviation of the flexural strength measurements of the sintered bodies are shown in Figure 6. Significant differences were detected among the measured strength values of the groups ( $P < .05$ ). A post hoc analysis confirmed that the ME group showed the highest mean strength value among the groups,  $752.63 \pm 237.57$  MPa ( $P < .05$ ). The LE group was reported to have the lowest value,  $370.38 \pm 44.15$  MPa, and the HE group was  $672.51 \pm 207.13$  MPa, with statistically significant difference ( $P$

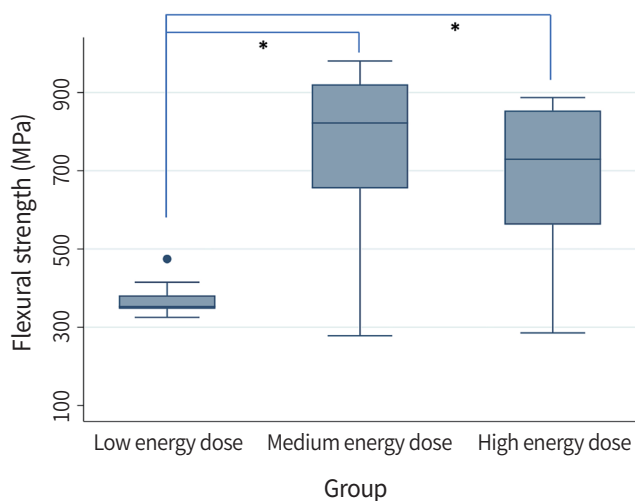


**Fig. 6.** Means and standard deviations of the flexural strength measurements of dental zirconia manufactured by digital light processing, under three different exposure energy conditions. Statistical significance was marked with an asterisk (\*).

$< .05$ ). However, there was no significant difference in the mean strength values between the ME and HE groups ( $P > .05$ ). Microscopic examination of the fractured surface confirmed that the specimen from the LE group had several micro-sized interlayer porosities and numerous agglomerates (Fig. 7). In the ME and HE groups, both specimens showed fewer agglomerates on the fractured surface than the LE group, and no distinctive interlayer pores or surface defects were detected in either group (Fig. 7).

## DISCUSSION

Based on these findings, the null hypothesis was rejected. The lateral resolution of the green body and flexural strength of the sintered body were the highest in the group with a medium dose of exposure energy. Because the dispersion stability of the zirconia suspension for up to 7-month period and the uniformity of the exposure intensity were consistent, and the layer thickness or recoating speed was controlled, the outcomes of the printed dental zirconia could be inferred to be mainly affected by the difference in the exposure energy dose during DLP. The resolution of 3D printing, either horizontal or vertical, is essential for layer-by-layer build-up of an object with sufficient accuracy. As displayed in Figure 8, it is essential to understand that the lateral resolution of the DLP-generated green body of dental zirconia could be affected by changes in the exposure energy dose.

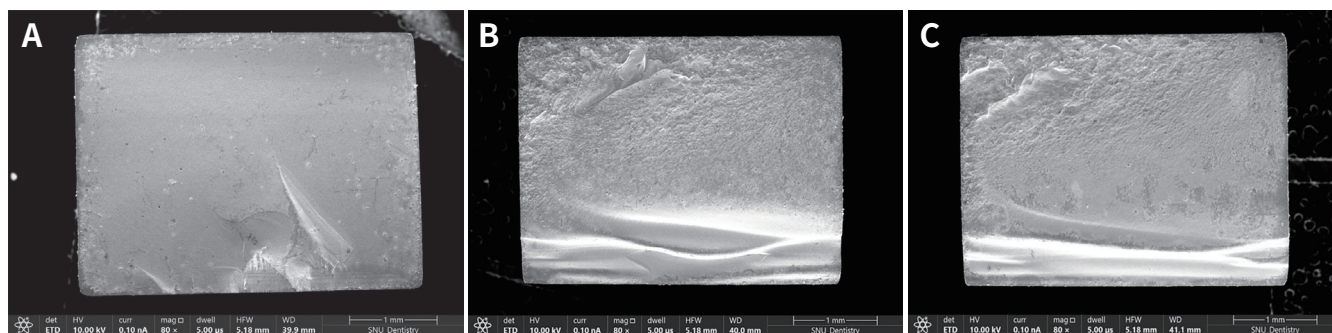


**Fig. 7.** Representative microscopic image of fractured dental zirconia specimens manufactured by digital light processing, under three different exposure energy conditions. (A) Low-energy group (LE), (B) Medium-energy group (ME), (C) High-energy group (HE). The LE group showed several micro-sized interlayer porosities and numerous agglomerates, while the ME and HE groups showed less agglomerates on the fractured surface than those of LE group, and had no distinctive interlayer pores or surface defects.

Regarding the lateral resolution, the cubic-shaped specimens showed all negative errors in the LE group and all positive errors in the HE group, implying that both the outline and isthmus widths were affected by scattering in the same trends. The linear dimensional change caused by the overgrowth of a printed green body has been reported differently depending on the shape of the printed object.<sup>10,16,23</sup> Overgrowth can be defined as the difference between the exposed and measured lengths of a green body, and most studies were conducted by measuring the width or diameter of the geometric shapes of hollow cubes or rings.<sup>10,16,23</sup> With high exposure energy, the oversized object showed a decreased hole diameter or gap width (negative deviation) in the hollow and an enlarged wall thickness or outer diameter (positive deviation) in the rim or ring.<sup>10,16,23</sup> However, these geometric shapes are too simple. In this study, a cubic shape with each top corner stacked identically with a small cube was used to imitate the molar tooth geometry and simplify the outline or isthmus width measurement. The different trends in the lateral resolution of the green bodies in these studies may be related to the different geometric shapes and dimensions of the printed objects.

The flexural strength of the sintered body can also be affected by decreasing or increasing the exposure energy, possibly owing to the quality of the green body. In this study, the strength of printed dental zir-

conia with a medium exposure energy dose was over 750 MPa, within the reported range of 200 - 800 MPa for zirconia produced by 3D printing.<sup>6,7</sup> Moreover, the lowest flexural strength was reported in the LE group, which may have originated from numerous micro-sized interlayer porosities and agglomerates. Internal flaws of the printed body, such as pores and agglomerations, have been suggested to increase the failure probability of zirconia.<sup>7,20,21</sup> High porosity can be related to the low fracture resistance of zirconia because the stress concentration and internal crack propagation around internal flaws can be detrimental to the structural integrity of zirconia.<sup>7,20,21</sup> In contrast to the LE group, the ME group exhibited no distinct interlayer pores or surface defects. Considering the equilibrium between interlayer adhesion by exposure and internal stress during photopolymerization within the green body, and the resultant structural integrity of the sintered zirconia (Fig. 9), it is critical to optimize the exposure energy in fabricating dental zirconia with DLP.

The dimensional deviation of printed zirconia depends on the exposure energy applied during DLP.<sup>6,10,23</sup> The ME group (150 mJ/cm<sup>2</sup>) was reported to have the most suitable dose for the zirconia suspension tested in terms of the lateral resolution of the green body and flexural strength of the sintered body. Similarly, for lithography-based ceramic manufacturing, one of the most studied DLP processes for

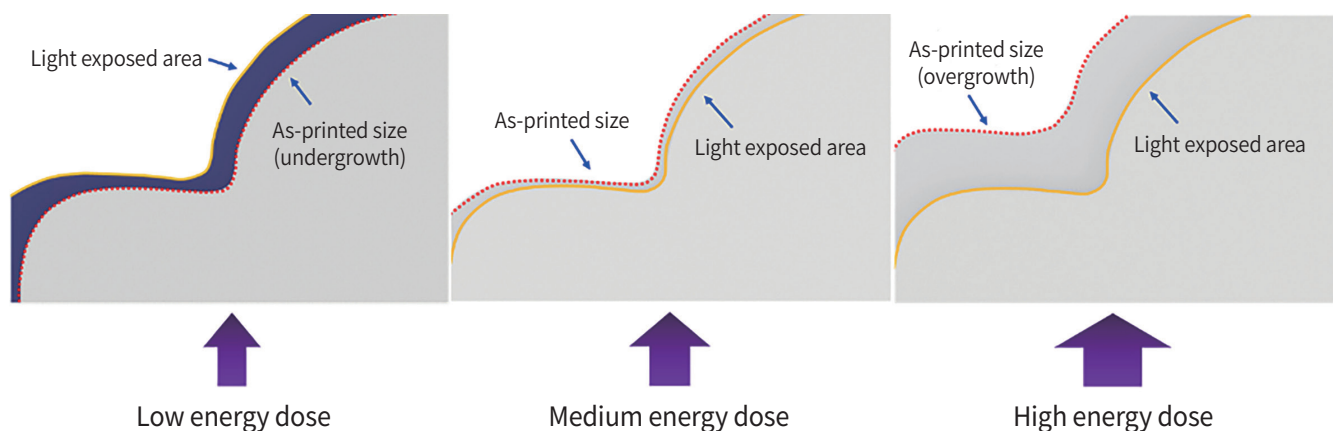


**Fig. 8.** Schematic diagram of association between overall exposure energy dose and lateral resolution of the zirconia green body (denoted as size difference between as-printed and light exposed area) fabricated by digital light processing.



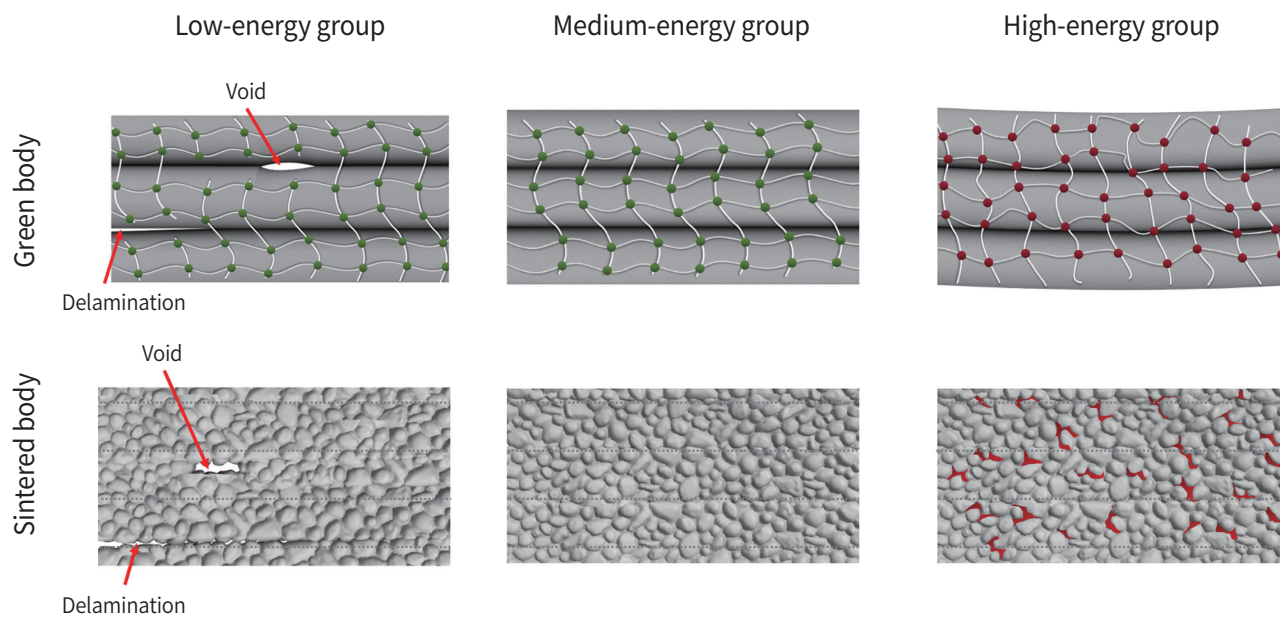


**Fig. 9.** Schematic diagram of association between the overall exposure energy dose and flexural strength of dental zirconia fabricated by digital light processing and post-processing. Note the layer structure of green body or sintered body can be different between the groups with different exposure energy dose, in terms of void and delamination (Low-energy group), or irregularity due to overgrowth and stress (High-energy group).

fabricating zirconia objects for dental applications, the exposure energy for the process recommended by the manufacturer was in the range of 110 - 190  $\text{mJ}/\text{cm}^2$ .<sup>19,23</sup> In accordance with the current findings, the lateral resolution of printed zirconia, including its diameters and thicknesses, decreased with an increase in exposure energy (higher than 150  $\text{mJ}/\text{cm}^2$ ) owing to intensified scattering-induced overgrowth.<sup>23</sup> A smaller exposure energy has been suggested for reducing the scattering effect of the green body dimension.<sup>6</sup> Because too low energy may not guarantee printability, the exposure energy for DLP should be monitored during printing to apply the printed zirconia for dental applications.<sup>23</sup>

This *in vitro* study revealed an association between the exposure energy dose during DLP using a digital workflow and the printed outcome quality (resolution and structural integrity) of dental zirconia at its green-body or sintered-body stages. The findings from this study contribute to the advancement of DLP in dental materials by defining the optimal setting of the exposure energy dose for the accuracy and mechanical strength of dental prostheses.

This study had several limitations. The dimension or shape of the printed specimen was simplified to measure the resolution, and the condition of the exposure energy may be different when producing dental crowns. The DLP printer tested in this study was developed for in-office dental prosthesis manufacturing, and the exposure energy value suggested to be optimal in this study may differ from those of other printers with different light sources or build-up mechanisms. Further studies on the various production parameters and printing mechanisms are required. To improve the clinical relevance of the results from the flexural strength test, a subtractively manufactured group may have to be added as a control group in order to compare the strengths of the additively manufactured groups.

## CONCLUSION

Given that the dispersion stability of the suspension and the uniformity of the light exposure intensity are guaranteed during the DLP process, the exposure energy dose of in-office manufacturing can affect the

lateral resolution of the green body and the flexural strength of the sintered body of zirconia for dental applications. Thus, it is important to optimize the exposure energy dose during DLP, considering that scattering-induced overgrowth can affect the adhesion between the layers. The flexural strength of sintered zirconia for dental applications may also be affected by changes in the exposure energy.

## REFERENCES

1. Alves MFRP, de Campos LQB, Simba BG, da Silva CRM, Strecker K, dos Santos C. Microstructural characteristics of 3Y-TZP ceramics and their effects on the flexural strength. *Ceramics* 2022;5:798-813.
2. Ayode Otitoju T, Ugochukwu Okoye P, Chen G, Li Y, Onyeka Okoye M, Li S. Advanced ceramic components: Materials, fabrication, and applications. *J Ind Eng Chem* 2020;85:34-65.
3. Chen F, Wu JM, Wu HQ, Chen Y, Li CH, Shi YS. Microstructure and mechanical properties of 3Y-TZP dental ceramics fabricated by selective laser sintering combined with cold isostatic pressing. *Int J Lightweight Mater Manuf* 2018;1:239-45.
4. Methani MM, Revilla-León M, Zandinejad A. The potential of additive manufacturing technologies and their processing parameters for the fabrication of all-ceramic crowns: A review. *J Esthet Restor Dent* 2020;32:182-92.
5. Cho JH, Yoon HI, Oh JH, Kim DH. Effect of maximum support attachment angle on intaglio surface trueness of anatomic contour monolithic prostheses manufactured by digital light processing and zirconia suspension. *J Prosthet Dent* 2023;129:478-85.
6. Meng J, Lian Q, Xi S, Yi Y, Lu Y, Wu G. Crown fit and dimensional accuracy of zirconia fixed crowns based on the digital light processing technology. *Ceram Int* 2022;48:17852-63.
7. Branco AC, Colaço R, Figueiredo-Pina CG, Serro AP. Recent advances on 3D-printed zirconia-based dental materials: a review. *Materials (Basel)* 2023;16:1860.
8. Kim YK, Yoon HI, Kim DJ, Han JS. Comparative analysis on intaglio surface trueness, wear volume loss of antagonist, and fracture resistance of full-contour monolithic zirconia crown for single-visit dentistry under simulated mastication. *J Adv Prosthodont* 2022;14:173-81.
9. Li R, Xu T, Wang Y, Sun Y. Accuracy of zirconia crowns manufactured by stereolithography with an occlusal full-supporting structure: An in vitro study. *J Prosthet Dent* 2022;S0022-3913(22)00064-6.
10. Mitteramskogler G, Gmeiner R, Felzmann R, Gruber S, Hofstetter C, Stampfl J, Ebert J, Wachter W, Laubersheimer J. Light curing strategies for lithography-based additive manufacturing of customized ceramics. *Addit Manuf* 2014;1-4:110-8.
11. Chaudhary R, Fabbri P, Leoni E, Mazzanti F, Akbari R, Antonini C. Additive manufacturing by digital light processing: a review. *Prog Addit Manuf* 2023;8:331-51.
12. Wu X, Teng J, Ji X, Xu C, Ma D, Sui S, Zhang Z. Research progress of the defects and innovations of ceramic vat photopolymerization. *Addit Manuf* 2023;65:103441.
13. Gentry SP, Halloran JW. Light scattering in absorbing ceramic suspensions: Effect on the width and depth of photopolymerized features. *J European Ceram Soc* 2015;35:1895-904.
14. Sun J, Binner J, Bai J. 3D printing of zirconia via digital light processing: optimization of slurry and debinding process. *J European Ceram Soc* 2020;40:5837-44.
15. Sun Y, Li M, Jiang Y, Xing B, Shen M, Cao C, Wang C, Zhao Z. High-quality translucent alumina ceramic through digital light processing stereolithography method. *Adv Eng Mater* 2021;23:2001475.
16. Yun Y, Deqiao X, Chen J, Zhaoling D, Lida S, Zongjun T, Yunfei C, Feng H. Mechanism of ceramic slurry light scattering affecting contour accuracy and method of projection plane correction. *Ceram Int* 2023;49:15024-33.
17. Zhang X, Wu X, Shi J. Additive manufacturing of zirconia ceramics: a state-of-the-art review. *J Mater Res Technol* 2020;9:9029-48.
18. Schweiger J, Bomze D, Schwentenwein M. 3D printing of zirconia-what is the future? *Curr Oral Health Rep* 2019;6:339-43.
19. Patil A, D DJ, Bomze D, Gopal V. Wear behaviour of lithography ceramic manufactured dental zirconia. *BMC Oral Health* 2023;23:276.
20. Xiang D, Xu Y, Bai W, Lin H. Dental zirconia fabricated by stereolithography: accuracy, translucency and mechanical properties in different build orientations. *Ceram Int* 2021;47:28837-47.
21. Zandinejad A, Das O, Barmak AB, Kuttolamadom

- M, Revilla-León M. The flexural strength and flexural modulus of stereolithography additively manufactured zirconia with different porosities. *J Prosthodont* 2022;31:434-40.
22. Bove A, Calignano F, Galati M, Iuliano L. Photopolymerization of ceramic resins by stereolithography process: a review. *Appl Sci* 2022;12:3591.
23. Conti L, Bienenstein D, Borlaf M, Graule T. Effects of the layer height and exposure energy on the lateral resolution of zirconia parts printed by lithography-based additive manufacturing. *Materials (Basel)* 2020;13:1317.